

Structural Basis for DNA Gyrase Interaction with Coumermycin A1

Arnaud Vanden Broeck,[†] Alastair G. McEwen,[†] Yasmine Chebaro,[†] Noëlle Potier,[‡] and Valérie Lamour^{*,†,§}

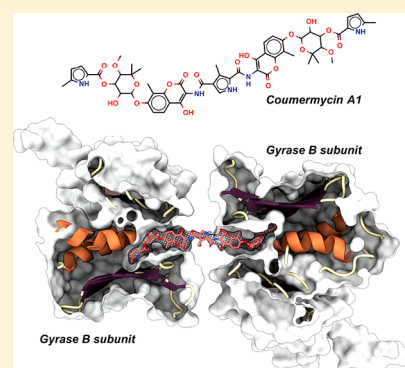
[†]Integrated Structural Biology Department, IGBMC, UMR7104 CNRS, U1258 Inserm, University of Strasbourg, Illkirch 67404, France

[‡]Laboratoire de Spectrométrie de Masse des Interactions et des Systèmes, UMR 7140 CNRS, University of Strasbourg, Strasbourg 67000, France

[§]Hôpitaux Universitaires de Strasbourg, Strasbourg 67000, France

Supporting Information

ABSTRACT: Coumermycin A1 is a natural aminocoumarin that inhibits bacterial DNA gyrase, a member of the GHKL proteins superfamily. We report here the first cocrystal structures of gyrase B bound to coumermycin A1, revealing that one coumermycin A1 molecule traps simultaneously two ATP-binding sites. The inhibited dimers from different species adopt distinct sequence-dependent conformations, alternative to the ATP-bound form. These structures provide a basis for the rational development of coumermycin A1 derivatives for antibiotherapy and biotechnology applications.



INTRODUCTION

Aminocoumarins are natural compounds secreted by *Streptomyces* sp. with antibacterial properties targeting GHKL ATPase binding sites and in particular that of the bacterial type IIA topoisomerase, DNA gyrase.^{1,2} The three representative aminocoumarins, novobiocin (NOV), clorobiocin (CLO), and coumermycin A1 (COU), share common chemical features (Figure 1). COU is a divalent aminocoumarin conjugate with two aminocoumarin moieties and two deoxy-L-noviose sugars.

The molecular interactions of aminocoumarins with the DNA gyrase ATP binding site have been well described from crystal structures with the exception of the COU.^{1,3–6} These structures showed that the deoxy-sugar of the aminocoumarins overlaps with the ATP binding site in the GyrB subunit, which is consistent with their being competitive inhibitors of ATP hydrolysis.⁷ Among the aminocoumarins, COU is the most potent antibiotic against DNA gyrase with an IC₅₀ lower than 6 nM against the pathogenic strain *Staphylococcus aureus*.⁸ Despite several *in vitro* studies on the inhibition of DNA gyrase by COU,^{7,9–14} the lack of structural information has impeded the detailed study of the molecular interaction with its targets and the development of more specific derivatives.

In the past 10 years, aminocoumarins have raised renewed interest due to increasing concern about antibiotic resistance¹⁵ and as potential remedies against cancer and HIV infections.^{16–19} With the discovery and the functional characterization of the aminocoumarins biosynthesis gene clusters,^{20,21} it is now possible to design new aminocoumarin analogues by

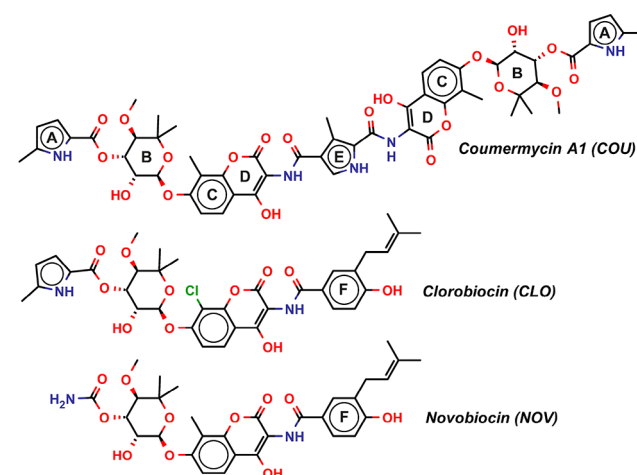


Figure 1. Chemical structure of aminocoumarins: (A) 5-methylpyrrolylcarbonyl; (B) deoxy-L-noviose sugar; (C, D) 4-hydroxycoumarin; (E) 2-4-pyrrolylcarbonyl; (F) benzamide moiety.

genetic engineering, such as mutagenesis, synthetic biology, or gene recombination.^{22,23} Additionally, the chemically induced dimerization of proteins fused to GyrB using a combination of COU/NOV has been developed for more than 20 years.²⁴ From the induced dimerization of Raf-1 kinases triggering

Received: December 7, 2018

Published: March 28, 2019

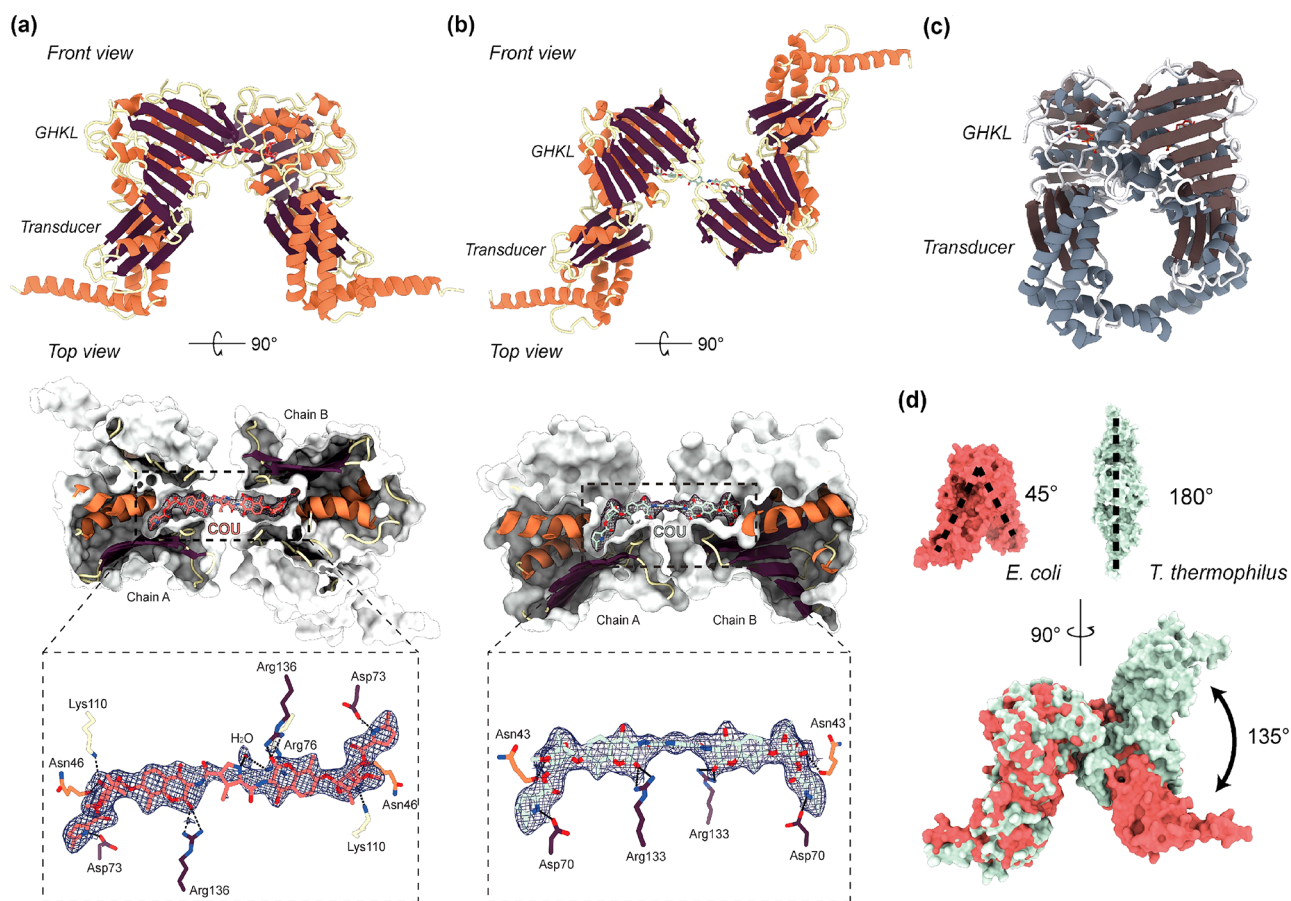


Figure 2. Crystal structures of *E. coli* (*Ec*) and *T. thermophilus* (*Tth*) GyrB 43K-coumermycin A1 complexes. (a) Front view of the *Ec* 43K-COU structure (PDB code 6ENG) showing a novel dimeric form in an inhibited state, different from the ATP- or NOV-bound homodimer. In the top view, a surface representation of the GHKL domain is sliced at the level of the COU molecule. The inset shows the $2F_o - F_c$ map at 1σ (blue grid) around COU molecules and hydrogen-bonds with conserved residues. (b) *Tth* 43K-COU structure (PDB code 6ENH). Coumermycin A1 (COU) is represented in pink (*Ec*) and pale green (*Tth*) sticks. (c) *Ec* 43K dimer structure in the presence of ADPNP displaying the ATPase sites to the outside of the structure. (d) Superimposition of the *Ec* and *Tth* 43K-COU structures. Upper panel is a side view of each COU-complexed structure in surface representation. Bottom panel is a front view of the two structures superimposition showing a 135° rotation of one of the monomers. The surfaces of *Ec* 43K-COU and *Tth* 43K-COU complexes are colored in orange and in green, respectively

cellular pathways²⁵ to the synthesis of drug-responsive hydrogels²⁶ or the negative selectable marker for selection of recombinant vaccinia virus,²⁷ these systems use COU as a switch-on chemical inducer. However, the lack of molecular details regarding the interaction of COU with GyrB limits the development of new biotechnology tools.

Herein, we report the first crystal structures of COU bound to the GHKL-transducer domains (43K) of *Escherichia coli* and *Thermus thermophilus* GyrB.

RESULTS AND DISCUSSION

The cocrystal structure of the *E. coli* (*Ec*) 43K-COU complex was solved by X-ray crystallography at 2.3 Å resolution (Table S1). The asymmetric unit contains two molecules forming a novel dimer in an inhibited state, different from the ATP- or NOV-bound homodimer^{3,28} (Figure 2a and Figure S2). The relative orientation of each monomer is different from the one found in structures of 43K fragments in complex with other aminocoumarins, in which novobiocin or clorobiocin binds the ATPase pockets with a 1:1 stoichiometry (Figure 2c). Instead, the ATPase sites of each subunit are facing each other, linked together by a unique COU molecule anchored in both ATPase sites with a 2:1 GyrB-COU stoichiometry (Figure 2a). As the

use of the 43K-COU entity is relevant for specific biotechnology applications requiring high temperatures, we also solved the crystal structure of the *T. thermophilus* (*Tth*) 43K-COU complex at 1.9 Å resolution (Table S1). The asymmetric unit contains only one 43K subunit but also forming an inhibited dimer with another subunit through crystallographic symmetry (Figure S2). A unique COU molecule is similarly anchored into both 43K ATPase sites that are also facing each other (Figure 2b). Surprisingly, the relative orientation of the monomers is different from that of the *Ec* complex (Figure 2d).

To confirm the stoichiometry of the complexes observed in the crystal structures, we used electrospray ionization time-of-flight (ESI-TOF) mass spectrometry. The native ESI mass spectrum provides a charge state distribution of the protein ions within a mass-overcharge (m/z) range. By deconvolution of the charge states (z), the mass (m) of the complexes was determined, and their stoichiometry was deduced. The results confirmed that the 43K fragments adopt a homodimeric form in the presence of only one molecule of COU, consistent with the stoichiometry observed in the crystal structures (Figure S3a and Table S2). Together, the crystal structures and mass spectrometry analysis provide direct evidence for the dimer

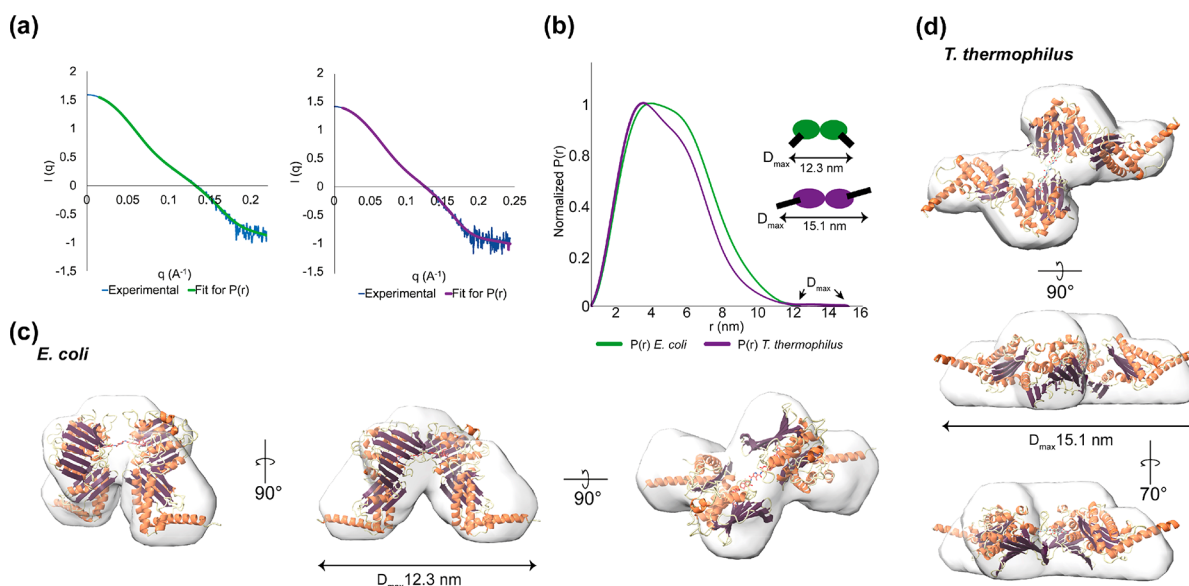


Figure 3. SAXS data and ab initio models of *Ec* and *Tth* GyrB 43K-COU complexes. (a) Experimental SAXS data of *Ec* (left) and *Tth* (right) 43K-COU complexes are represented in blue. Green and purple curves represent the fit of the $P(r)$ functions in reciprocal space on the experimental SAXS data of *Ec* and *Tth* complexes, respectively. (b) Normalized $P(r)$ functions (pair-distance distribution) of the *Ec* and *Tth* 43K-COU complex in their respective colors. The schemes in inset represent the potential shape of the complex in solution based on the $P(r)$ function curve and on the D_{\max} . (c) Fit of the *Ec* 43K-COU complex X-ray structure (PDB code 6ENG) in the ab initio model calculated with DAMMIF³⁰ presented in different orientations. (d) Fit of the *Tth* 43K-COU complex X-ray structure (PDB code 6ENH) in the ab initio model calculated with DAMMIF³⁰ presented in different orientations.

formation and COU stoichiometry, in agreement with earlier biochemical and isothermal calorimetry analysis.^{7,9} The mechanism by which COU binds with a 1:2 stoichiometry may explain why this divalent antibiotic retains the best IC₅₀ value against DNA gyrase compared to novobiocin and clorobiocin.^{14,29} Interestingly, some *E. coli* strains have developed an unusual resistance mechanism using the overexpression of WT GyrB to overcome subunit sequestration by COU, further illustrating its peculiar inhibition mode.¹²

The superimposition of one monomer of each of the two shows a 135° rotation of the second monomer (Figure 2d). The two different conformations of the 43K-COU revealed by the structures raise questions about the possible conformations of the complexes in solution. We first performed size exclusion chromatography experiments with the 43K domains alone and in complex with COU (Figure S3b). The elution profile confirmed the formation of dimers in the presence of COU for both species but with a difference in the elution shift (1.76 and 0.78 mL, respectively), suggesting different hydrodynamic radii for *Ec* and *Tth*, potentially indicative of distinct conformations in solution (Table S2).

To analyze more precisely the conformations of the complexes in solution, we performed small angle X-ray scattering (SAXS) measurements coupled to size-exclusion chromatography (Figure S4a). The data processing of the experimental scattering curves (Figure 3a) provides different valuable parameters of the complexes in solution: the radius of gyration (R_g), which is defined as the root-mean-square distance of all scattering elements of a molecule from their center of mass (a measure of the overall shape of a molecule), and the maximal distance (D_{\max}), which is the maximum length of the molecule in solution. Interestingly, we observed clear differences in the R_g and D_{\max} for the *Ec* and *Tth* 43k-COU complexes (R_g of 3.64 and 3.40 nm; D_{\max} of 12.3 and 15.1 nm, respectively) (Table S2). We then calculated for each complex

the pair-distance distribution function ($P(r)$), which describes the paired-set of all distances between points within a molecule. The $P(r)$ for the *Ec* complex is consistent with a dual-core shaped molecule with small flexible ends, while the *Tth* function depicts a single core with more elongated extremities (Figure 3b). Then, using the SAXS experimental data, we were able to compute low-resolution envelopes of the complexes. The degree of similarity between the X-ray structures and the in-solution envelopes was assessed by cross-correlation (CC). High CC scores were obtained for both complexes (*Ec*, 0.89; *Tth*, 0.9), showing a very good fit between the solution and crystal structures (Figure 3c,d). In addition, rigid-body modeling of the monomers against the solution scattering data resulted in dimeric models adopting conformations very close to those of the X-ray structures (Figure S4c). These results confirm that the different conformations of the complexes observed in the X-ray structures are the same in solution and not triggered by crystal contacts.

The complete COU molecule could be fitted in the electron density of both structures (Figure 2a,b). The COU molecule features dual and extended arms which bind identically to each ATPase site of the GyrB monomers. Most of the contacts with the protein are made through these arms leaving the central 2-4-pyrrolylcarbamoyl group free of interaction, except for the *Ec* complex where one water molecule interacts with the nitrogen atom of the central pyrrole and the Arg76 of the B subunit (Figure 4a). The majority of the interactions stabilizing the COU inside the ATPase pocket of *Ec* and *Tth* 43K GyrB are similar to those described in the crystal structure of *Ec* 24K GyrB with clorobiocin.^{4,5} The *Tth* Ala117, whose equivalent in *Ec* is Val120, weakly contributes to hydrophobic stabilization of COU in the pocket (Figure 4 and Figure S5). Additional interactions in the *Ec* 43K-COU structure can be observed compared with the GyrB 24K structures with novobiocin and

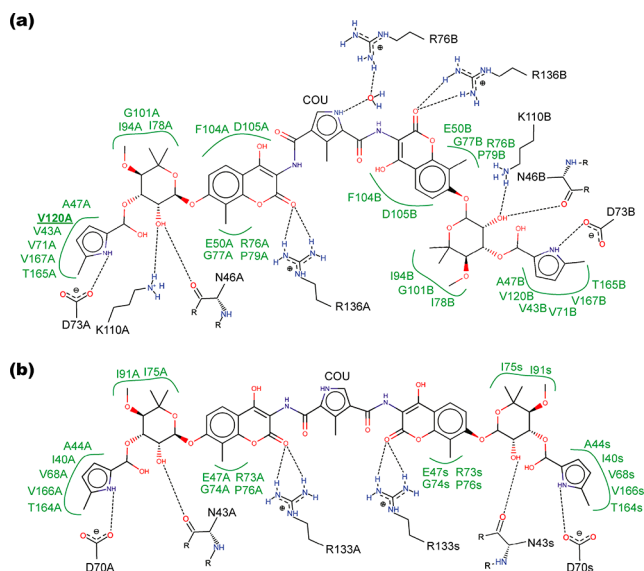


Figure 4. Identification of residues interacting with coumermycin A1. Two-dimensional representation of the interaction network (a) in the *E. coli* 43K-COU structure (PDB code 6ENG) and (b) in the *T. thermophilus* 43K-COU structure (PDB code 6ENH). Hydrogen bonds are represented by dashed lines. Green residues are interacting through hydrophobic contacts.

clorobioicin, due to the stabilization of the highly dynamic ATP lid by crystal contacts (Figure 4 and Figure S6). In particular, the side chains of Phe104 and Asp105 make hydrophobic interactions with the coumarin ring. In the *Tth* 43K-COU structure, the counterpart residues could not be built in the model due to the absence of electronic density in the map. However, it is interesting to note that the ATP lid adopts a different conformation in the *Ec* 43K-COU complex compared to the *Tth* 43K-novobiocin³ structure, where both ATP lids could be built. This difference is most likely due to the position of the benzamide moiety group of novobiocin that pushes back the ATP lid into a more open position (Figure S6).

The structures of the gyrase complexes with COU now provide molecular details for the analysis of resistance mutations. In particular, D89G, a common mutation found in novobiocin-resistant *S. aureus* strains, decreases 8-fold the affinity for novobiocin compared to a WT strain.³¹ In contrast, COU binding is reduced only by 2-fold with the same mutant strains. This can be explained by the absence of the phenolic moiety in COU which does not contact the Asp89 residue. Instead, the central pyrrole is not stabilized by any interaction with residues in both structures (Figure 4). Similarly, a COU-resistant *S. aureus* resistant strain was reported to harbor three mutations (Q136E, I175T, L455I) in GyrB.³¹ The mutation of Ile175, a residue close to the pyrrolamide, into threonine leads to a 4-fold decrease in COU binding. It can be explained by the change of polarity in the binding pocket, conferring an unfavorable interaction (Figure S7a). Residues Q136E and L455I are positioned far away from the COU binding site and should have little effect on the binding of the drug (Figure S7a,b).

The major difference between the conformation of the COU molecules in the *Ec* and *Tth* structures lies in the carbonyl groups surrounding the central pyrrole moiety. They adopt either a *cis* or *trans* conformation that seems to dictate the relative position of the extended arms (Figure S8a,b). To

probe if alternative conformations for the COU are accessible, we performed ab initio geometry optimizations in order to explore the minimum energy conformations. The calculated local minima are very close to their respective starting points, and both have similar energies (−3886.7 au), indicating that both *cis* and *trans* conformations of the COU are stable conformations (Figure S8a,b). Besides, ab initio calculations show that the two isomeric forms are stabilized by the hydrogen bonds between the carbonyls surrounding the central pyrrole and the hydroxyl groups located on the amino-coumarin rings (Figure S8c,d).

The distance between the protein monomers is determined by the ~10 Å spacing of the two hydroxyl groups of each COU 4-hydroxycoumarin moiety (Figure 4 and Figure 5). As a

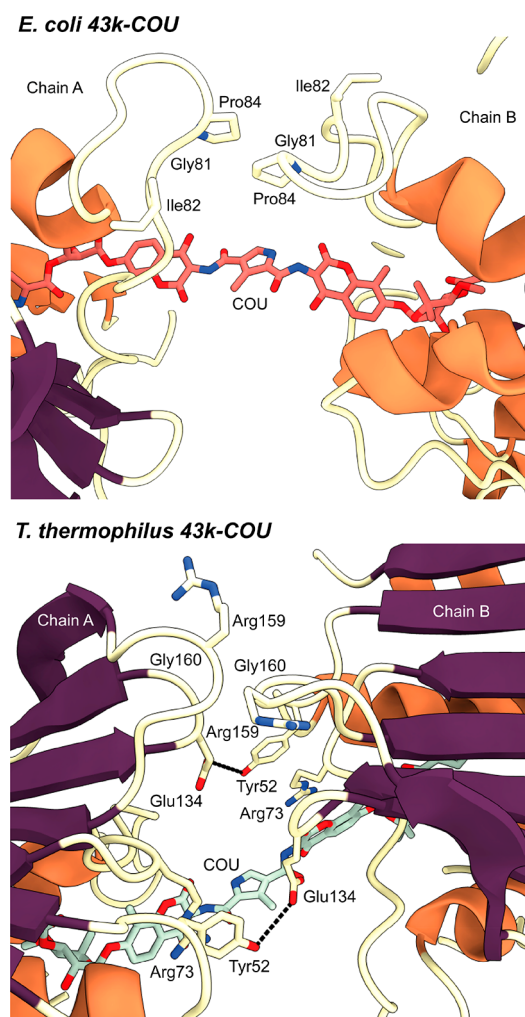


Figure 5. Dimeric interface of the GyrB 43K-COU complexes. The *Ec* dimer is stabilized by three residues in each chain, Gly81, Ile82, and Pro84. The *Tth* dimer is stabilized by five residues on each monomer: Arg159, Gly160, Tyr52, Glu134, and Arg73. COU is colored in salmon and pale green, respectively. Hydrogen bonds are represented by dashed black lines.

consequence, few residues at the surface are involved in the stabilization of the monomers' orientation. They form interfaces of only 69.2 and 131.1 Å² for the *Ec* and *Tth* complexes, respectively. However, their significant solvation-free gain energies are consistent with an interaction specific interface (Table S3). The *Ec* dimer is stabilized by three

residues in each chain, Gly81, Ile82, and Pro84 which are involved in hydrophobic interactions (Figure 5a). The *Tth* dimer is stabilized by five residues on each monomer. Residues Arg159 and Gly160 are engaged in hydrophobic interactions, and residue Tyr52 on one monomer forms a hydrogen bond with Glu134 positioned on the other monomer. Residue Tyr52 also forms a π -stack interaction with COU and Arg73 (Figure 5b). It is noteworthy that none of the residues involved in the interfaces of the two complexes are strictly conserved and that they are located on flexible loops (Figure S9). For instance, residue Tyr52 in the *Tth* complex is replaced by His55 in *Ec* (Figure S9). By extension, if the *Ec* complex adopts the *Tth* dimer conformation, residue His55 would remain too far from the conserved Glu137 (*Tth* Glu134), positioned on the other monomer, to form a hydrogen bond (Figure 5b). Hence, the *Ec* 43K-COU complex would not be stabilized in the conformation adopted by the *Tth* dimer. Intriguingly, residues Arg159 and Gly160, inserted in the primary sequence of *Tth* GyrB, are not present in five other representatives of Gram-negative (*E. coli*, *S. enterica*) or Gram-positive (*B. subtilis*, *S. aureus*, *M. tuberculosis*) bacteria (Figure S9). These two residues, involved in hydrophobic interactions at the dimer interface, strengthen the contacts between the monomers. As they are absent in *Ec*, this further explains why the dimer cannot adopt the conformation of the *Tth* complex. This analysis suggests that each conformation is driven by patterns of species-specific residues at the surface interface. It also shows that despite the distance between the monomers imposed by the COU itself, a few residues are sufficient to stabilize the dimer conformations. To take advantage of these different interfaces, chemical derivation of the central pyrrole or the surrounding carbonyls could be performed to specifically trigger contacts between COU and surface residues of a pathogen of interest. Furthermore, to increase the effectiveness of such symmetric compound like COU, it would become interesting to design dimeric drugs that can target two different proteins harboring GHKL domains as for example Topo IV, the other bacterial type II topoisomerase.

We have also evaluated the interaction of DNA gyrase per se (GyrB₂A₂ holoenzyme) and its different subunits (GyrB and GyrA) with COU by size-exclusion chromatography. Our results show that the complete GyrB subunit dimerizes in the presence of COU the same way as the GyrB 43K fragment. Addition of COU to the GyrA subunit does not induce any change to its elution volume. Strikingly, a bigger complex than the DNA gyrase holoenzyme is formed in the presence of reconstituted gyrase (GyrB₂A₂) and COU. The stoichiometry of this complex is likely to be GyrB₄A₂ based on a calibration curve. Interestingly, the trapped GyrB₂-COU complex supplemented with GyrA subunit is also able to form a complex whose elution volume is identical to the GyrB₂A₂ + COU, likely to be GyrB₄A₂ (Figure S10). Overall, these results suggest that the GyrB₄A₂ complex can be formed in two different ways: (a) an already formed gyrase holoenzyme is inhibited by COU, where the free aminocoumarin fragment of the drug captures another GyrB yielding a GyrB₄A₂ complex; (b) two COU-trapped GyrB dimers associate with two GyrA subunits to form a GyrB₄A₂ complex (Figures S10 and S11). In both cases, the DNA gyrase activity is impaired. In the context of resistance to COU by GyrB subunit overexpression,¹² it is likely that the resistance is maintained due to the capture of COU by the overexpressed free GyrB subunits, preventing any binding of COU to the active gyrase.

Aminocoumarins have been shown to interact with other ATP-binding GHKL fold-containing proteins³² and in particular the eukaryotic heat shock protein Hsp90,^{19,33} an emerging target in anticancer therapies. COU inhibits Hsp90 10-fold greater than novobiocin.³⁴ Furthermore, new COU analogues have been reported to harbor antiproliferative activity and IC₅₀ values against Hsp90 100-fold more potent than the natural molecule.³⁵ It has been shown that COU disrupts the Hsp90 dimer. The disruption thus prevents the binding between Hsp90 and several important cochaperones.³⁶ The X-ray structures of COU bound to GyrB (Figure 2) now provide atomic parameters crucial for further improvement of docking studies involving COU and Hsp90 or its other targets.^{18,34} Furthermore, the ab initio calculations provide a more detailed overview of the COU conformational landscape in silico, also contributing to the structure-guided discovery of new COU-related inhibitors against HSP90 (Figure S8).^{36–38}

The proven efficacy of COU to trigger dimerization of proteins of interest fused to the GyrB subunit has been demonstrated.^{24–26} However, it is difficult to estimate the success rate of this dimer induction strategy. Here, we provide a rational structural basis to design and improve biotechnology tools using COU. By using the GyrB subunit from *E. coli* or from *T. thermophilus*, it becomes possible to impose a 45° or 180° angle between the monomers fused to proteins of interest for the induction of distinct cellular effects (Figure S12). The 45° angle may be used to bring together two protein partners in order to induce their dimerization. On the other hand, the 180° angle could help with connecting large molecules and avoiding steric clashes. The 180° geometry also becomes relevant to trigger binding of a protein of interest to the cell membrane through the COU-induced dimerization of a GyrB-fusion attached to a membrane protein. Additionally, we showed that *Tth* 43K is stable at high temperatures with a T_m of 88.4 °C and that the complex with COU increases stability to a T_m of 90.1 °C (Figure S13 and Table S2). Using *Tth* 43K for specific biotechnology applications demanding high temperatures, such as polymer self-assembling polypeptide bionanomaterials³⁹ or heat-resistant hydrogels,²⁶ now becomes relevant.

CONCLUSIONS

We solved the X-ray structures of *E. coli* and *T. thermophilus* GyrB 43K in complex with coumermycin A1, revealing the molecular details of this divalent antibiotic sequestering an alternative inhibited dimer. Our structures show that one coumermycin A1 molecule binds two GyrB subunits in different conformations depending on the species. These structural data provide a rationale for structure-guided chemical modifications of coumermycin A1 that will facilitate the design of new molecules with better affinity and specificity toward DNA gyrase from pathogenic strains or other protein targets. It also sets the ground for improvement of biotechnology tools using coumermycin A1.

ASSOCIATED CONTENT

Supporting Information

The Supporting Information is available free of charge on the ACS Publications website at DOI: 10.1021/acs.jmedchem.8b01928.

Experimental section; tables for crystallographic data collection and refinement statistics, biophysical charac-

terization of GyrB 43K-COU complexes and PISA analysis; figures showing biochemical and biophysical characterization of the GyrB 43K-COU complex and DNA gyrase-COU complex, analysis of the structures with regard to COU mutant strains, ab initio calculation of COU, model for the in vivo interaction of DNA gyrase with COU, and supporting biotechnological usage of COU (PDF)

Molecular formula string for coumermycin A1 (CSV)

Accession Codes

Coordinates and structure factors have been deposited: accession codes 6ENG and 6ENH. Authors will release the atomic coordinates upon article publication.

AUTHOR INFORMATION

Corresponding Author

*E-mail: lamourv@igbmc.fr.

ORCID

Valérie Lamour: 0000-0001-7793-4029

Author Contributions

A.V.B. and V.L. conceived the study and designed the experiments. A.V.B., A.G.M., Y.C., and N.P. performed the experiments. A.V.B., A.G.M., Y.C., N.P., and V.L. analyzed and interpreted the data. A.V.B. and V.L. wrote the manuscript.

Notes

The authors declare no competing financial interest.

ACKNOWLEDGMENTS

We acknowledge SOLEIL and the European Synchrotron Radiation Facility for provision of synchrotron radiation facilities. We thank Leonard Chavas for assistance on beamline Proxima 1, Christophe Mueller-Dieckmann on beamline ID30B, and Petra Pernot on beamline BM29. We thank Anna Belorusova for her help with the SAXS experiments, and Alexandra Cousido-Siah and Alberto Podjarny for suggestions on X-ray data processing. This work was supported by the Fondation ARC and Grant ANR-10-LABX-0030-INRT (managed by the Agence Nationale de la Recherche under the frame program Investissements d'Avenir Grant ANR-10-IDEX-0002-02). The authors acknowledge the support and the use of resources of the French Infrastructure for Integrated Structural Biology Grant FRISBI ANR-10-INBS-05 and of Instruct-ERIC. Computational resources were provided by the Méso-Centre de Calcul (University of Strasbourg).

ABBREVIATIONS USED

Ec, *Escherichia coli*; *Tth*, *Thermus thermophilus*; NOV, novobiocin; CLO, clorobiocin; COU, coumermycin A1; 43K, GyrB ATPase-transducer domain; ESI-TOF, electrospray ionization time-of-flight; D_{max} , maximum distance; R_g , gyration radius; $P_{(r)}$, pair-distance distribution function; T_m , denaturation midpoint

REFERENCES

(1) Collin, F.; Karkare, S.; Maxwell, A. Exploiting bacterial DNA gyrase as a drug target: current state and perspectives. *Appl. Microbiol. Biotechnol.* **2011**, *92*, 479–497.
(2) Bush, N. G.; Evans-Roberts, K.; Maxwell, A. DNA topoisomerases. *EcoSal Plus* **2015**, *6*, 6.
(3) Lamour, V.; Hoermann, L.; Jeltsch, J. M.; Oudet, P.; Moras, D. An open conformation of the *Thermus thermophilus* gyrase B ATP-binding domain. *J. Biol. Chem.* **2002**, *277*, 18947–18953.

(4) Lafitte, D.; Lamour, V.; Tsvetkov, P. O.; Makarov, A. A.; Klich, M.; Deprez, P.; Moras, D.; Briand, C.; Gilli, R. DNA gyrase interaction with coumarin-based inhibitors: the role of the hydroxybenzoate isopentenyl moiety and the 5'-methyl group of the noviose. *Biochemistry* **2002**, *41*, 7217–7223.

(5) Tsai, F. T.; Singh, O. M.; Skarzynski, T.; Wonacott, A. J.; Weston, S.; Tucker, A.; Pauptit, R. A.; Breeze, A. L.; Poyser, J. P.; O'Brien, R.; Ladbury, J. E.; Wigley, D. B. The high-resolution crystal structure of a 24-kDa gyrase B fragment from *E. coli* complexed with one of the most potent coumarin inhibitors, clorobiocin. *Proteins: Struct., Funct., Genet.* **1997**, *28*, 41–52.

(6) Lewis, R. J.; Singh, O. M.; Smith, C. V.; Skarzynski, T.; Maxwell, A.; Wonacott, A. J.; Wigley, D. B. The nature of inhibition of DNA gyrase by the coumarins and the cyclothialidines revealed by X-ray crystallography. *EMBO J.* **1996**, *15*, 1412–1420.

(7) Ali, J. A.; Jackson, A. P.; Howells, A. J.; Maxwell, A. The 43-kilodalton N-terminal fragment of the DNA gyrase B protein hydrolyzes ATP and binds coumarin drugs. *Biochemistry* **1993**, *32*, 2717–2724.

(8) Alt, S.; Mitchenall, L. A.; Maxwell, A.; Heide, L. Inhibition of DNA gyrase and DNA topoisomerase IV of *Staphylococcus aureus* and *Escherichia coli* by aminocoumarin antibiotics. *J. Antimicrob. Chemother.* **2011**, *66*, 2061–2069.

(9) Gormley, N. A.; Orphanides, G.; Meyer, A.; Cullis, P. M.; Maxwell, A. The interaction of coumarin antibiotics with fragments of DNA gyrase B protein. *Biochemistry* **1996**, *35*, 5083–5092.

(10) Gellert, M.; O'Dea, M. H.; Itoh, T.; Tomizawa, J. Novobiocin and coumermycin inhibit DNA supercoiling catalyzed by DNA gyrase. *Proc. Natl. Acad. Sci. U. S. A.* **1976**, *73*, 4474–4478.

(11) Hooper, D. C.; Wolfson, J. S.; McHugh, G. L.; Winters, M. B.; Swartz, M. N. Effects of novobiocin, coumermycin A1, clorobiocin, and their analogs on *Escherichia coli* DNA gyrase and bacterial growth. *Antimicrob. Agents Chemother.* **1982**, *22*, 662–671.

(12) del Castillo, I.; Vizan, J. L.; Rodriguez-Sainz, M. C.; Moreno, F. An unusual mechanism for resistance to the antibiotic coumermycin A1. *Proc. Natl. Acad. Sci. U. S. A.* **1991**, *88*, 8860–8864.

(13) Samuels, D. S.; Garon, C. F. Coumermycin A1 inhibits growth and induces relaxation of supercoiled plasmids in *Borrelia burgdorferi* the Lyme disease agent. *Antimicrob. Agents Chemother.* **1993**, *37*, 46–50.

(14) Fedorko, J.; Katz, S.; Allnoch, H. In vitro activity of coumermycin A1. *Appl. Microbiol.* **1969**, *18*, 869–873.

(15) Hooper, D. C.; Jacoby, G. A. Mechanisms of drug resistance: quinolone resistance. *Ann. N. Y. Acad. Sci.* **2015**, *1354*, 12–31.

(16) Hong, D. S.; Banerji, U.; Tavana, B.; George, G. C.; Aaron, J.; Kurzrock, R. Targeting the molecular chaperone heat shock protein 90 (Hsp90): lessons learned and future directions. *Cancer Treat. Rev.* **2013**, *39*, 375–387.

(17) Chen, N. Y.; Zhou, L.; Gane, P. J.; Opp, S.; Ball, N. J.; Nicastro, G.; Zufferey, M.; Buffone, C.; Luban, J.; Selwood, D.; Diaz-Griffero, F.; Taylor, I.; Fassati, A. HIV-1 capsid is involved in post-nuclear entry steps. *Retrovirology* **2016**, *13*, 28.

(18) Vozzolo, L.; Loh, B.; Gane, P. J.; Tribak, M.; Zhou, L.; Anderson, I.; Nyakatura, E.; Jenner, R. G.; Selwood, D.; Fassati, A. Gyrase B inhibitor impairs HIV-1 replication by targeting Hsp90 and the capsid protein. *J. Biol. Chem.* **2010**, *285*, 39314–39328.

(19) Yu, X. M.; Shen, G.; Neckers, L.; Blake, H.; Holzbeierlein, J.; Cronk, B.; Blagg, B. S. Hsp90 inhibitors identified from a library of novobiocin analogues. *J. Am. Chem. Soc.* **2005**, *127*, 12778–12779.

(20) Wang, Z. X.; Li, S. M.; Heide, L. Identification of the coumermycin A1 biosynthetic gene cluster of *Streptomyces rishiriensis* DSM 40489. *Antimicrob. Agents Chemother.* **2000**, *44*, 3040–3048.

(21) Steffensky, M.; Muhlenweg, A.; Wang, Z. X.; Li, S. M.; Heide, L. Identification of the novobiocin biosynthetic gene cluster of *Streptomyces spheroides* NCIB 11891. *Antimicrob. Agents Chemother.* **2000**, *44*, 1214–1222.

(22) Heide, L. The aminocoumarins: biosynthesis and biology. *Nat. Prod. Rep.* **2009**, *26*, 1241–1250.

(23) Wolpert, M.; Heide, L.; Kammerer, B.; Gust, B. Assembly and heterologous expression of the coumermycin A1 gene cluster and production of new derivatives by genetic engineering. *ChemBioChem* **2008**, *9*, 603–612.

(24) Rutkowska, A.; Schultz, C. Protein tango: the toolbox to capture interacting partners. *Angew. Chem., Int. Ed.* **2012**, *51*, 8166–8176.

(25) Farrar, M. A.; Alberola-Ila, J.; Perlmutter, R. M. Activation of the Raf-1 kinase cascade by coumermycin-induced dimerization. *Nature* **1996**, *383*, 178–1781.

(26) Ehrbar, M.; Schoenmakers, R.; Christen, E. H.; Fussenegger, M.; Weber, W. Drug-sensing hydrogels for the inducible release of biopharmaceuticals. *Nat. Mater.* **2008**, *7*, 800–804.

(27) White, S. D.; Conwell, K.; Langland, J. O.; Jacobs, B. L. Use of a negative selectable marker for rapid selection of recombinant vaccinia virus. *BioTechniques* **2011**, *50*, 303–309.

(28) Brino, L.; Urzhumtsev, A.; Mousli, M.; Bronner, C.; Mitschler, A.; Oudet, P.; Moras, D. Dimerization of *Escherichia coli* DNA-gyrase B provides a structural mechanism for activating the ATPase catalytic center. *J. Biol. Chem.* **2000**, *275*, 9468–9475.

(29) Confreres, A.; Maxwell, A. *gyrB* mutations which confer coumarin resistance also affect DNA supercoiling and ATP hydrolysis by *Escherichia coli* DNA gyrase. *Mol. Microbiol.* **1992**, *6*, 1617–1624.

(30) Franke, D.; Svergun, D. I. DAMMIF, a program for rapid ab-initio shape determination in small-angle scattering. *J. Appl. Crystallogr.* **2009**, *42*, 342–346.

(31) Phillips, J. W.; Goetz, M. A.; Smith, S. K.; Zink, D. L.; Polishook, J.; Onishi, R.; Salowe, S.; Wiltsie, J.; Allocco, J.; Sigmund, J.; Dorso, K.; Lee, S.; Skwish, S.; de la Cruz, M.; Martin, J.; Vicente, F.; Genilloud, O.; Lu, J.; Painter, R. E.; Young, K.; Overbye, K.; Donald, R. G.; Singh, S. B. Discovery of kibelomycin, a potent new class of bacterial type II topoisomerase inhibitor by chemical-genetic profiling in *Staphylococcus aureus*. *Chem. Biol.* **2011**, *18*, 955–965.

(32) Dutta, R.; Inouye, M. GHKL, an emergent ATPase/kinase superfamily. *Trends Biochem. Sci.* **2000**, *25*, 24–28.

(33) Burlison, J. A.; Neckers, L.; Smith, A. B.; Maxwell, A.; Blagg, B. S. Novobiocin: redesigning a DNA gyrase inhibitor for selective inhibition of hsp90. *J. Am. Chem. Soc.* **2006**, *128*, 15529–15536.

(34) Cele, F. N.; Kumalo, H.; Soliman, M. E. Mechanism of inhibition of Hsp90 dimerization by gyrase B inhibitor coumermycin A1 (C-A1) revealed by molecular dynamics simulations and thermodynamic calculations. *Cell Biochem. Biophys.* **2016**, *74*, 353–363.

(35) Kusuma, B. R.; Peterson, L. B.; Zhao, H.; Vielhauer, G.; Holzbeierlein, J.; Blagg, B. S. Targeting the heat shock protein 90 dimer with dimeric inhibitors. *J. Med. Chem.* **2011**, *54*, 6234–6253.

(36) Allan, R. K.; Mok, D.; Ward, B. K.; Ratajczak, T. Modulation of chaperone function and cochaperone interaction by novobiocin in the C-terminal domain of Hsp90: evidence that coumarin antibiotics disrupt Hsp90 dimerization. *J. Biol. Chem.* **2006**, *281*, 7161–7171.

(37) Burlison, J. A.; Blagg, B. S. Synthesis and evaluation of coumermycin A1 analogues that inhibit the Hsp90 protein folding machinery. *Org. Lett.* **2006**, *8*, 4855–4858.

(38) Byrd, K. M.; Subramanian, C.; Sanchez, J.; Motiwala, H. F.; Liu, W.; Cohen, M. S.; Holzbeierlein, J.; Blagg, B. S. Synthesis and biological evaluation of novobiocin core analogues as Hsp90 inhibitors. *Chem. - Eur. J.* **2016**, *22*, 6921–6931.

(39) Doles, T.; Božič, S.; Gradišar, H.; Jerala, R. Functional self-assembling polypeptide bionanomaterials. *Biochem. Soc. Trans.* **2012**, *40* (4), 629–634.